Synthesis, Antimalarial Activity, and Molecular Modeling of Tebuquine Analogues

Paul M. O'Neill,* David J. Willock,*,† Shaun R. Hawley, Patrick G. Bray, Richard C. Storr,† Stephen A. Ward, and B. Kevin Park

Departments of Chemistry and of Pharmacology and Therapeutics, The University of Liverpool, P.O. Box 147, Liverpool L69 3BX, U.K.

Received May 23, 1996[⊗]

Tebuquine (**5**) is a 4-aminoquinoline that is significantly more active than amodiaquine (**2**) and chloroquine (**1**) both *in vitro* and *in vivo*. We have developed a novel more efficient synthetic route to tebuquine analogues which involves the use of a palladium-catalyzed Suzuki reaction to introduce the 4-chlorophenyl moiety into the 4-hydroxyaniline side chain. Using similar methodology, novel synthetic routes to fluorinated (**7a**,**b**) and a dehydroxylated (**7c**) analogue of tebuquine have also been developed. The novel analogues were subjected to testing against the chloroquine sensitive HB3 strain and the chloroquine resistant K1 strain of *Plasmodium falciparum*. Tebuquine was the most active compound tested against both strains of *Plasmodia*. Replacement of the 4-hydroxy function with either fluorine or hydrogen led to a decrease in antimalarial activity. Molecular modeling of the tebuquine analogues alongside amodiaquine and chloroquine reveals that the inter-nitrogen separation in this class of drugs ranges between 9.36 and 9.86 Å in their isolated diprotonated form and between 7.52 and 10.21 Å in the heme−drug complex. Further modeling studies on the interaction of 4-aminoquinolines with the proposed cellular receptor heme revealed favorable interaction energies for chloroquine, amodiaquine, and tebuquine analogues. Tebuquine, the most potent antimalarial in the series, had the most favorable interaction energy calculated in both the *in vacuo* and solvent-based simulation studies. Although fluorotebuquine (**7a**) had a similar interaction energy to tebuquine, this compound had significantly reduced potency when compared with (**5**). This disparity is possibly the result of the reduced cellular accumulation (CAR) of fluorotebuquine when compared with tebuquine within the parasite. Measurement of the cellular accumulation of the tebuquine analogues and seven related 4-aminoquinolines shows a significant relationship ($r = 0.98$) between the CAR of 4-aminoquinoline drugs and the reciprocal of drug IC_{50}.

Introduction

It is estimated that over 40% of the world's population is exposed to the risk of malaria at any one time and that there are an estimated 2 million deaths associated with the disease per year.[1] A number of chemical classes of drugs have been investigated for the treatment of malaria; these include the 8-aminoquinolines, quinolinemethanols, sulfonamides, and dihydrofolate reductase inhibitors. However in terms of the extent of use and their clinical success, the most important class of drugs to be used for the treatment of malaria are the 4-aminoquinolines such as chloroquine (**1**) (Chart 1). The development of chloroquine resistance by *Plasmodium falciparum* has underlined the requirement for alternative drugs which are effective against resistant strains. Since amodiaquine (**2**) is a 4-aminoquinoline antimalarial that is active against certain resistant strains of *P. falciparum*, we have undertaken a detailed investigation of the pharmacology and structure−activity relationships (SAR) of analogues in this class.

Chemically amodiaquine differs from chloroquine in that it contains a *p*-hydroxyanilino aromatic ring in its side chain. This structural change would be expected to alter not only the lipophilicity and pK_a of the two basic nitrogen atoms[2] but also the conformational flexibility of the side chain. Thus, although both amodiaquine and chloroquine have four carbon atoms between their 4-amino and terminal alkylamino nitrogen atoms, the incorporation of the aryl function in amodiaquine would be expected to impart greater structural rigidity. Structural elaboration of amodiaquine by further chemical substitution in the aryl ring has led to compounds with improved antimalarial activity against sensitive and resistant strains. Following the observation that compounds **3** and **4** had potent antimalarial activity, Werbel examined a series of hybrid structures of **4** and amodiaquine in the hope that incorporation of the 7-chloroquinoline moiety would enhance activity further.[3] A range of amodiaquine analogues containing aryl functionality at the 3′-position were synthesized and a QSAR study was used to establish the most suitable substituents on the aryl ring. From this study it was shown that optimal activity was achieved with 4-chlorophenyl substitution and *tert*-butyl substitution in the side chain. Tebuquine (**5**) was shown to be the most potent analogue in the series and was selected for preclinical toxicology studies prior to evaluation in man.

Tebuquine (**5**) contains the 4-aminophenol moiety and therefore would be expected to undergo P450-mediated oxidation to a toxic quinonimine in a similar manner to amodiaquine.[4−6] We have recently shown that the isosteric replacement of the 4-hydroxyl function in amodiaquine with fluorine produced an amodiaquine analogue (**6**) which had antimalarial activity against chloroquine resistant and sensitive *P. falciparum*.[7] Furthermore, this analogue was not susceptible to

† Department of Chemistry.
[⊗] Abstract published in *Advance ACS Abstracts,* January 1, 1997.

S0022-2623(96)00370-6 CCC: $14.00

Chart 1. Structures of 4-Aminoquinoline Antimalarials

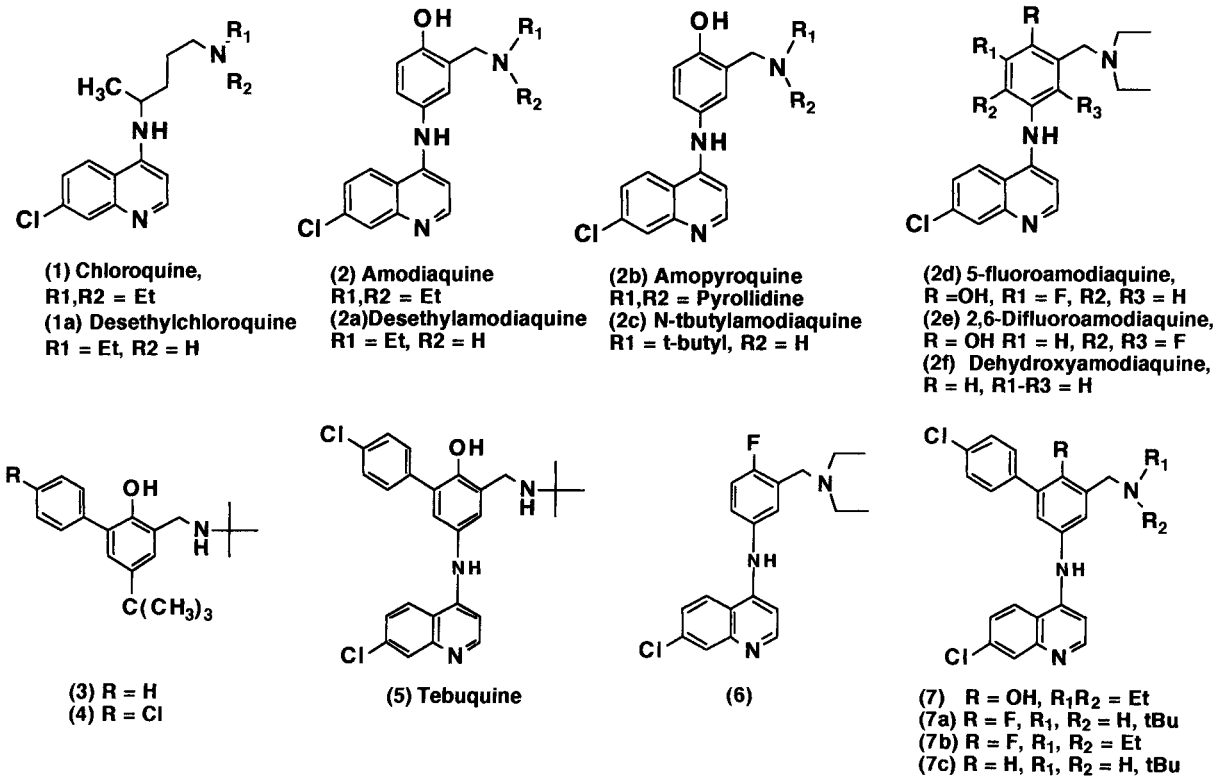

bioactivation to a toxic quinonimine.[8−10] More recently we have shown that incorporation of fluorine into the 8-aminoquinoline antimalarial primaquine can reduce toxicity without affecting antimalarial potency. In this particular example, fluorine was used to prevent the formation of toxic quinonimines by oxidative metabolism.[11] In the present study we have explored the effect on antimalarial activity of replacing the 4-hydroxyl function of tebuquine with either fluorine or hydrogen and with *tert*-butyl or diethylamino substitution in the side chain (**7**−**7c**).[12] It was proposed that simple chemical changes of this type would provide compounds with high antimalarial activity with potentially lower toxicity. The novel analogues were subjected to testing *in vitro* against the chloroquine sensitive HB3 strain and the chloroquine resistant K1 strain of *P. falciparum*.

Several lines of evidence suggest that the mechanism of activity of aminoquinolines involves interference with the hemoglobin degradation pathway. In particular it has been suggested that a target for 4-aminoquinolines such as chloroquine and amodiaquine is ferriprotoporphyrin IX ("heme").[13−15] Therefore using MOPAC, a molecular modeling study into the range of possible conformations for each drug molecule was carried out, and using force field techniques, the interaction of these novel agents with ferriprotoporphyrin IX was investigated. The results obtained for tebuquine and its analogues were compared with data obtained for amodiaquine and chloroquine. In particular we were interested to examine the effects of chemical substitution on the energy and on which functional groups are involved in the heme-binding interaction. The results obtained were then examined along with differences in cellular accumulation in order to rationalize the range of antimalarial potencies of the analogues under test.[16]

Scheme 1. Synthesis of Tebuquine[a]

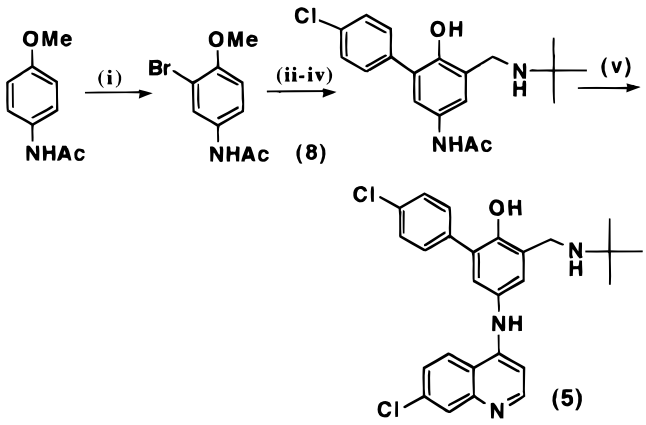

[a]Reagents: (i) Br_2, AcOH (ii) $Pd(PPh_3)_4$, Cl-⟨⟩-$B(OH)_2$ Na_2CO_3 (iii) BBr_3, CH_2Cl_2 (iv) CH_2O, t-$BuNH_2$ (v) 40% HCl, 4,7DQ

Chemistry

Since we wished to compare the antimalarial activity of the novel compounds against tebuquine and its diethylamino analogue amotebuquine (**7**), we devised the novel synthetic route shown in Scheme 1. The most critical challenge involved in this synthesis was preparation of the requisite 4-chlorophenyl-substituted 4-hydroxyacetanilide. Werbel investigated two routes to this intermediate. The first approach utilized the Ullman reaction and gave low yields of the required intermediate.[17] An alternative approach involved the use of the Hill reaction, and this gave good yields of 3-(4′-chlorophenyl)-4-hydroxyacetanilide.[18] In spite of the good yields obtained by this route, the starting materials for this synthesis (e.g., sodium nitromalonaldehyde) are not commercially available. We decided to investigate an alternative approach to **5** from 3-bromo-4-methoxyac-

Scheme 2. Synthesis of Fluorotebuquine[a]

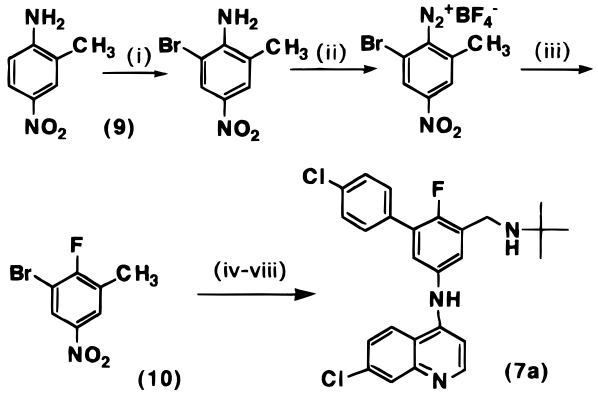

[a] Reagents: (i) Br_2, AcOH; (ii) HNO_2, HBF_4; (iii) Δ, 150 °C; (iv) Suzuki coupling, $Pd^0(PPh_3)_4$, toluene, 4-chlorophenylboronic acid, 2 M Na_2CO_3, Δ; NBS, AIBN, CCl_4, Δ; (vi) RNH_2; (vii) Sn, HCl; (viii) 4,7-dichloroquinoline, ethanol, reflux.

Scheme 3. Synthesis of Dehydroxytebuquine[a]

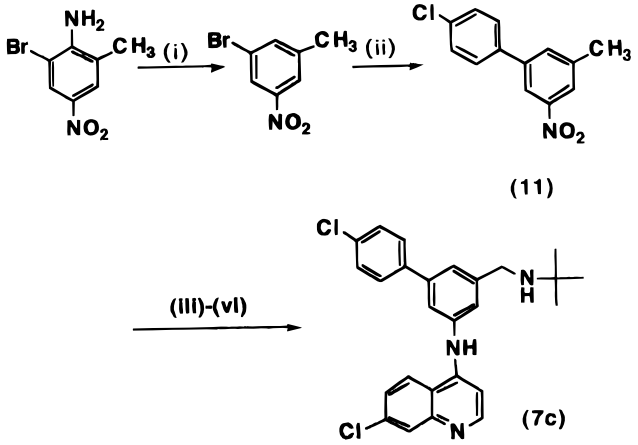

[a] Reagents: (i) HNO_2, H+; (ii) Suzuki coupling, $Pd^0(PPh_3)_4$, toluene, 4-chlorophenylboronic acid, 2 M Na_2CO_3, Δ; (iii) NBS, AIBN, CCl_4; Δ (iv) t-$BuNH_2$, toluene; (v) Sn, HCl; (vi) 4,7-dichloroquinoline, ethanol, reflux.

etanilide[19] using the Suzuki reaction[20] of **8**. In this reaction 3-bromo-4-methoxyacetanilide was allowed to react with 4-chlorophenylboronic acid in the presence of tetrakis(triphenylphosphine)palladium ($Pd^0(PPh_3)_4$) and 2 M sodium carbonate to give the required product, 3-(4′-chlorophenyl)-4-methoxyacetanilide, in excellent yield (80%). Boron tribromide-catalyzed demethylation led to the required phenol in high overall yield (68%). The phenol was subsequently subjected to a Mannich reaction to give the required aminoalkyl compound. Hydrolytic removal of the amide function and coupling with 4,7-dichloroquinoline gave tebuquine (**5**). The corresponding diethylamino analogue, amotebuquine (**7**), was synthesized as for tebuquine except that diethylamine was used in the Mannich reaction.

The required intermediate **10** for the synthesis of fluorotebuquine was obtained by the Balz−Schiemann reaction of 2-amino-3-bromo-5-nitrotoluene which was prepared in turn by the bromination of 2-amino-5-nitrotoluene (**9**). Compounds containing the nitro group are known to decompose rapidly and violently in the Schiemann reaction; the severity of the reaction can be limited by diluting the diazonium salt with an inert additive such as acid-washed sand, anhydrous sodium carbonate, barium sulfate, or sodium fluoride. Yields are also increased if an inert gas such as nitrogen is flushed through the apparatus during decomposition since this limits contact of the BF_3 with product and hence side reactions and tar formation. The required diazonium salt (Scheme 2) was synthesized by standard procedures and mixed with acid-washed sand. Decomposition at 150 °C under a constant flow of nitrogen gave the required intermediate **10** in 50% yield following flash column chromatography to remove tar and decomposition products. The fluoro product was then subjected to the palladium-catalyzed Suzuki reaction, and the resulting compound was brominated with AIBN/NBS to give the required bromomethyl compound.

Further transformations as shown in Scheme 2 gave the required fluoro derivative **7a**. The corresponding diethylamino analogue, fluoroamotebuquine (**7b**), was also synthesized by this route.

Scheme 3 shows the route utilized for the preparation of dehydroxytebuquine. 2-Amino-3-bromo-5-nitrotoluene was deaminated by reaction with sodium nitrite in acid. The deaminated product was then allowed to react in the palladium-catalyzed Suzuki reaction as for fluorotebuquine to give **11**. Bromination, nucleophilic displacement of bromide by *tert*-butylamine, reduction, and coupling furnished the required product **7c** in good overall yield.

Table 1. *In Vitro* Activity of Tebuquine Analogues

drug	HB3 IC_{50} (nM)	SD ± mean	K1 IC_{50} (nM)	SE ± mean
chloroquine (**1**)	9.75	2.7	250	7.1
amodiaquine (**2**)	3.7	0.8	27.2	4.3
tebuquine (**5**)	0.9	0.3	20.8	1.4
amotebuquine (**7**)	24.2	1.8	42.1	3.6
fluorotebuquine (**7a**)	61.6	4.1	74.3	1.4
fluoroamotebuquine (**7b**)	104.1	4.7	101.3	6.8
dehydroxytebuquine (**7c**)	56.6	1.8	74.2	3.2

Antimalarial Activity

Two strains of *P. falciparum* from Thailand were used in this study: (a) the uncloned K1 strain which is known to be chloroquine resistant and (b) the HB3 strain which is chloroquine sensitive. Table 1 compares the activity[21,22] for the various analogues. It is immediately apparent that replacement of the hydroxyl function in tebuquine with fluorine results in a reduction in antimalarial activity. Isosteric replacement of the hydroxyl function of tebuquine with fluorine to give fluorotebuquine results in a 4-fold loss of activity. Replacement of the *tert*-butyl function in fluorotebuquine with a diethylamino function results in a further loss in antimalarial potency. In spite of these comparative losses in activity, both fluorotebuquine (**7a**) and fluoroamotebuquine (**7b**) are more potent than chloroquine against the chloroquine resistant K1 strain of the parasite. Removal of the hydroxyl function in tebuquine also leads to a loss in antimalarial potency. Dehydroxytebuquine (**7c**) was significantly less potent than tebuquine (**5**) or amodiaquine (**2**) in the HB3 strain of the parasite. In the chloroquine resistant strain dehydroxytebuquine had similar activity to fluorotebuquine (**7a**).

Full experimental details for the calculation of the cellular accumulation ratio (CAR) of 4-aminoquinolines is described by Hawley et al.[2] The CAR values for **1**, **1a**, **2**, **2a**−**f**, **5**, **6**, and **7a**) obtained in the HB3 sensitive strain of the parasite are shown in Table 5.

Molecular Modeling

Molecular modeling was carried out in order to test an earlier hypothesis[23] that the inter-nitrogen separation (quinoline N to alkylamino N) is an important factor for drug activity. These earlier studies were carried out using the MMX force field[24] and *single energy-minimized structures* were used for the determination of the inter-nitrogen separation. A simplified receptor model was also developed and compared with the minimized molecular structures, since the authors did not put forward a specific receptor. From our experimental studies we believe that the antimalarial agents' mode of action involves binding to heme. Accordingly we have generated energy-minimized molecular conformations for a representative set of the compounds studied and then calculated their likely interaction with heme. In addition, in the former study, energy minimization calculations were carried out using the monoprotonated form of the drug (i.e., protonation on the diethylamino nitrogen in chloroquine and amodiaquine). Since the site of action of 4-aminoquinolines is believed to be in the acidic food vacuole of the parasite (pH = 5.5),[13,42] we have concentrated on the diprotonated forms of the drug in our modeling studies. To emphasize the importance of solution pH on conformation, calculations were also carried out on the unprotonated molecules for comparison. To examine dynamic effects in the presence of solvent, we have also carried out simulations with a discrete water model for selected heme−drug complexes and the isolated drug molecules. This progression of simulation methods are dealt with in turn below.

All molecular modeling was carried out on an Indigo 2 R4000 silicon graphics workstation. Simulation studies were carried out on chloroquine, amodiaquine, tebuquine (**5**), fluorotebuquine (**7a**), and dehydroxytebuquine (**7c**). Each molecule was energy minimized from the "as constructed" conformation using the extensible systematic force field (ESFF)[25] and the Discover program.[26] The ESFF force field has been developed by MSI and is able to parameterize a much wider range of atom types than earlier force fields. The approach uses a simple set of atomic parameters which are expanded to a larger set according to the atomic environment. The parameters and rules have been developed from fitting to density functional calculation results, experimental data, and X-ray structure information. This parameter set has recently been used to successfully model the structure and interactions of oligomers of iron-containing poly(ferrocenylsilanes).[27]

Energy minimization alone is only able to find the nearest energy minimum to the starting conformation of any system. In order to generate a wider representative set, many techniques have been developed including simple graphical alignment of molecules to give "likely" structures[28] and molecular dynamics to generate sets of starting points from thermodynamic ensembles of structures. In our studies we have employed the method of simulated annealing, an approach similar to that recently empolyed by Milne.[29] Molecular dynamics (MD) runs at 298 K for a simulation time of 5 ps were performed for each drug molecule, and the resulting structure was energy minimized to gain a low-energy conformation. This process was repeated until 10 structures per molecule had been generated. For each MD calculation, the last minimized structure in the set was used as the next starting point. One potential disadvantage of the molecular mechanics approach is the arbitary energy zero used in defining the interatomic potentials. For this reason each of the structures was finally minimized using the MOPAC semiempirical Hartree−Fock code (PM3 Hamiltonian, restricted spin states). From this procedure 10 molecular conformations were generated which would be expected to exist at the MD simulation temperature of 298 K. This number gave a sufficiently wide range of molecular conformations to show that each molecule could adopt structures which had inter-nitrogen distances spanning that expected from the earlier study. The thermally averaged inter-nitrogen separation can be calculated using the equation:

$$\langle R \rangle = \frac{\sum_i R_i \exp(-(E_i - E_m))/kT}{\sum_i \exp(-(E_i - E_m))/kT}$$

where E_i and E_m are the i^{th} and minimum calculated heats of formation for this molecule, respectively, R is the inter-nitrogen separation, and kT is the usual Boltzman factor (T = 298 K used throughout). Values of $\langle R \rangle$ are listed in Table 2. In all cases we observe that the mean inter-nitrogen atom separations are increased and the spread of calculated distances is greatly narrowed on diprotonation of the molecules studied.

This corresponds to the electrostatic repulsion between the protonated sites which gives rise to an effective stretching force. The narrowing of the distributions may be expected to increase the concentration of molecular conformations near the mean in low-pH enviroments. Having generated a set of conformations for each molecule, an investigation into their interactions with the heme unit was carried out. A model of heme (ferriprotoporphyrin IX) was constructed with a single hydroxy group ligating the Fe atom above the ring (see, for example, the heme unit in Figure 4). This unit was then energy minimized with the ESFF potential set and a net molecular charge of −e. Two possible conformations were considered as follows: (i) with the carboxylic acid groups on opposite sides of the porphyrin ring (as in Figure 4a) and (ii) with these groups on the same side of the ring. The latter conformation was found to be 2.3 kcal mol^{-1} lower in energy than the

Table 2. Effect of Diprotonation on the Inter-Nitrogen Separation of 4-Aminoquinolines

	av N−N (Å)	range of N−N (Å)
Molecules *in Vacuo* without Protonation		
chloroquine (**1**)	7.28	5.7−9.3
amodiaquine (**2**)	8.87	6.9−9.9
5′-fluoroamodiaquine (**2d**)	8.94	7.0−9.5
dehydroxyamodiaquine (**2f**)	7.40	7.1−9.7
tebuquine (**5**)	8.68	6.0−9.5
fluorotebuquine (**7a**)	7.85	7.0−9.7
dehydroxytebuquine (**7c**)	8.52	7.2−9.7
Molecules *in Vacuo* with Diprotonation		
chloroquine (**1**)	9.36	8.4−10.4
amodiaquine (**2**)	9.45	8.2−9.9
5′-fluoroamodiaquine (**2d**)	9.86	7.8−10.0
dehydroxyamodiaquine (**2f**)	9.38	7.8−9.9
tebuquine (**5**)	9.56	9.4−9.9
fluorotebuquine (**7a**)	9.65	8.9−9.9
dehydroxytebuquine (**7c**)	9.37	9.2−9.8

Table 3. Comparison of Antimalarial Activity with Heme-Binding Energies and Inter-Nitrogen Separation

drug	HB3 IC_{50} (nM)	N−N (Å)	interaction energy (kcal mol^{-1})
chloroquine (**1**)	9.75	7.52	−43.544
amodiaquine (**2**)	3.7	10.21	−13.573
tebuquine (**5**)	0.9	9.89	−58.58
fluoroamodiaquine (**6**)	31.9	10.18	−11.25
fluorotebuquine (**7a**)	61.6	9.37	−47.42
dehydroxytebuquine (**7c**)	56.6	10.04	−4.94

former due to an internal hydrogen bond (OH···OC = 1.83 Å). Both minimizations successfully reproduced the expected small out-of-plane displacement of the Fe on the opposite side of the ring to its hydroxy ligand.

From the 10 structures for each molecule generated by the MOPAC simulations of the diprotonated molecules above, we chose the lowest energy structure which was then used to generate a complex of drug molecules and heme in the following manner. From NMR data[30,31] we expected each molecule to π-stack with the quinoline ring above the π-system of the porphyrin. With this restriction each molecule was positioned over the heme model in such a way that the quaternary-charged nitrogen atom was within 3−4 Å of a carboxylic acid oxygen atom on the heme molecule. From this starting point we then energy minimized each dimer again using the ESFF parameter set. It was expected that these starting points would encourage hydrogen bonding between the quaternary nitrogen protons and the carboxylic acid groups. Each drug molecule was docked in this way with both heme conformations (see above) in turn, and several alternative starting points were investigated.

The interaction energy,[32] E_I, for each heme complex was then calculated from the equation:

$$E_I = E_D - E_M - E_H$$

where E_D is the lowest complex energy obtained and E_M and E_H are the lowest energies calculated for any conformation of the molecule and heme unit in isolation. Note that although the intramolecular energy terms are arbitrarily zero referenced in molecular mechanics force fields, the use of this definition of the interaction energy effectively contains only changes in conformational energy and inter-molecular interactions (which in our case are represented with Lennard−Jones repulsion dispersion potentials and electrostatic interactions). This means that it is valid to compare energies between different molecular structures. A similar approach to this has been employed by Rodighiero et al. in a recent molecular modeling study of Psoralen analogues.[28] The lowest interaction energies found for each molecule are tabulated in Table 3.

Following the initial studies, we then examined the effect of solvent by conducting longer molecular dynamics runs (100 ps) in the presence of a discrete water model. The complex structures generated in the vacuum were solvated by generating a sphere of water around the dimer centered on an atom in the middle of the molecular pair and with a radius of 14 Å. This was sufficient in all cases to give a layer of water of at least 5 Å around both molecules. The starting point for the heme−tebuquine (R═OH) structure is shown in Figure 5. These structures where then energy minimized

Table 4. Inter-Nitrogen Separation and Interaction Energies of Solvated 4-Aminoquinolines

	av N−N (Å)	range of N−N (Å)	rel interaction energy (kcal mol^{-1})
Solvated Molecules in Isolation			
tebuquine (**5**)	9.53	8.6 - 10.4	
dehydroxytebuquine (**7c**)	6.99	5.6−8.7	
amodiaquine (**2**)	8.56	6.7−10.4	
dehydroxyamodiaquine (**2f**)	9.91	8.4−10.7	
Solvated Heme−Drug Complex			
tebuquine (**5**)	9.38	8.1−10.2	−231.3
dehydroxytebuquine (**7c**)	9.34	8.1−10.1	−131.8
amodiaquine (**2**)	10.13	9.4−10.6	−149.9
dehydroxyamodiaquine (**2f**)	9.88	8.7−10.6	−148.7

followed by a molecular dynamics equilibration period of 5 ps, at 298 K. The results discussed here were generated from a further 100 ps molecular dynamics run again at 298 K. Every 0.5 ps during this simulation the atom coordinates were archived allowing geometric analysis to be performed later. To generate the isolated drug molecule energies, we simply cut out the heme molecule from the complex, the void being filled with solvent molecules during the equilibration time of the molecular dynamics.

These calculations were considerably more costly in terms of computer time than those for the *vacuo* case (taking around 10 days of wall time per calculation), and so we reduced the data set to four key molecules: tebuquine (**5**), dehydroxytebuquine (**7c**), amodiaquine, and dehydroxyamodiaquine (**2f**). The total energy of the system was averaged based on each 1 fs time step as the simulation proceeded. This remained virtually constant with a typical standard deviation of 1.5% in the total energy. In Table 4 we include a relative interaction energy which is the difference in total energy of the heme−drug complex and the solvated drug molecule alone.

The use of longer MD time scales also allowed us to examine dynamic effects on the drug-binding interaction. For instance in the case of amodiaquine it was found that the solvated molecule has a much narrower range of N−N distances in the heme complex structure than when in isolation (Table 4). This can be understood from the time dependence of the molecular geometry during the MD runs. In Figure 1a the N−N distance for amodiaquine is plotted as a function of time using the archived "snapshots" from the MD run. In the isolated molecule this shows a bimodal behavior with the separation switching between around 8 and 10 Å over a relatively short time period. We also show the time dependence of the CCNC dihedral angle (Figure 1b); this is formed with the axis of rotation along the quinoline C to bridging N atom bond such that for a 0° angle the quinoline and phenyl rings are coplanar. This bimodal behavior, with the angle changing sign, indicates that the two rings have passed through the unstable coplanar arrangement. In the amodiaquine−heme complex case we find that this transition never occurs during the simulation showing that the interaction with the heme molecule limits the available drug conformations to the longer N−N distances (Table 4).

Discussion

The aims of the study were to investigate the chemical basis of the antimalarial activity of 4-aminoquinolines

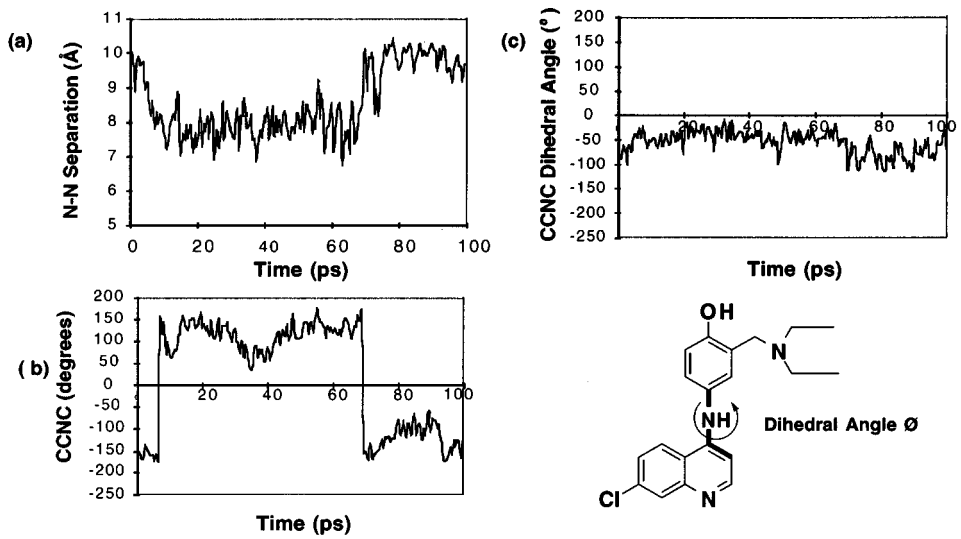

Figure 1. Dynamic effects on the amodiaquine drug binding interaction: (a and b) the calculated N−N distances and CCNC dihedral angle, amodiaquine alone; (c) the CCNC dihedral angle for amodiaquine in the solvated heme dimer.

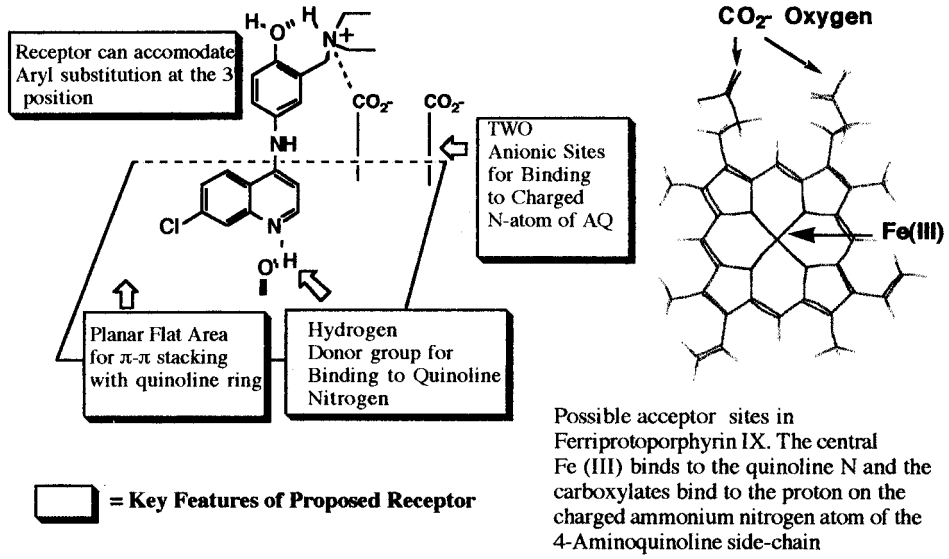

Figure 2. Pharmacophoric groups of 4-aminoquinolines and features of the proposed receptor. The figure on the left illustrates features of the receptor proposed by Koh et al.[23] with a comparison of the structure of ferriprotoporphyrin IX.

such as tebuquine (**3**), with particular respect to the potential for interacting with "heme" and the ability to accumulate within the parasite. Recent studies by Koh have demonstrated that the antimalarial drug amodiaquine can adopt a "bioactive conformation" with an inter-nitrogen ($N_{quin}-N_{diethyl}$) separation of 8.30 Å.[23,33] This distance is similar to the inter-nitrogen separation in the related antimalarial chloroquine ($N_{quin}-N_{diethyl}$ = 8.38 Å). It was suggested that the "bioactive conformation" and hence inter-nitrogen separation in amodiaquine is dependent on an intramolecular hydrogen bond between the hydroxyl function and the proton on the charged nitrogen in the diethylamino side chain. In this study Koh assumed that only the side chain nitrogen was protonated, and it was suggested that the pharmacophore for aminoquinolines related to amodiaquine is as shown in Figure 2. The "4-aminoquinoline receptor" was proposed to consist of a planar flat region to accommodate the quinoline ring and an additional two carboxylates in its structure.

As a direct result of hemoglobin metabolism, in the food vacuole of the parasite "heme" (ferriprotoporphyrin IX) is produced which has been proposed to be toxic to the parasite. Soluble heme can inhibit various enzymes, disrupt membrane function,[34] and promote lipid peroxidation.[35] In order to survive the parasite must remove the heme, and this is achieved by its conversion into an insoluble, unreactive crystalline material known as hemozoin.[36,37] Complexes of a drug with ferriprotoporphyrin IX could prevent incorporation of heme into hemozoin resulting in the observed toxic effects.[38] Since the complexes of chloroquine and ferriprotoporphyrin IX can lyse membranes, the aminoquinoline−heme complexes[39] have been proposed as the causative cytotoxic agents. Furthermore, since these complexes can only be formed in malaria-infected red cells, they are good candidates for accounting for the selective toxicity of aminoquinolines such as amodiaquine and chloroquine. The aminoquinoline−heme complexes can also cross membranes and reach targets outside the digestive vacuole.[40]

We suggest that the proposed receptor suggested by Koh is in fact ferriprotoporphyrin IX (heme, FPIX) since FPIX has a planar flat region of 30−40 Å to accommodate the flat quinoline ring, a central acceptor iron atom that can potentially bind to the quinoline nitrogen and two anionic carboxylates that can bind to the charged nitrogen of the aminoquinoline side chain (Figure 2). Furthermore, we might expect the potential acceptor sites on the receptor (the central ferric iron atom and the carboxylate oxygens) to have similar interatomic distances to the donor atoms in the drug, i.e., $N_{quin}-N_{diethyl} = 8.30$ Å (monoprotonated) and $N_{quin}-N_{diethyl} = 9-10$ Å (diprotonated). X-ray crystallographic measurements of the distance between the central iron atom and the oxygens in the carboxylates of heme are around 8.20 Å.[41] Thus it appeared that a two-point interaction may be possible in the "heme−drug complex" (although it should be noted that since interaction of the proton on the terminal nitrogen N_{alkyl} with the carboxylate oxygens will be of a hydrogen-bonding nature, the inter-nitrogen separation values of a given aminoquinoline need not match that closely the heme iron−oxygen separation). Notably if heme is the target for 4-aminoquinolines the binding model would accommodate the large *p*-chlorophenyl function at the 3′-position in tebuquine.

Table 2 gives the inter-nitrogen separation ($N_{quin}-N_{alkyl}$) of the diprotonated species. Diprotonation of amodiaquine and tebuquine results in an intramolecular separation ($N_{quin}-N_{side\ chain}$) of 9.1−10 Å and raises the overall energy of the molecule under investigation. A comparison of inter-nitrogen separation of the isolated drug molecules with antimalarial activity in the analogues demonstrates that there is no obvious relationship as previously suggested.[23] This factor is important since it rules out rationale design of antimalarials based simply on this parameter.

It was proposed that the differences in activity observed in this study in the chloroquine sensitive HB3 strain may be on account of changes in the interaction of the tebuquine analogues with heme. The chloroquine sensitive strain was selected for comparison with heme interaction energies since comparison with data from the resistant strain is complicated by the expression of a P-glycoprotein exporter that might be expected to reduce the steady state concentrations of analogues reaching the food vacuole and hence interacting with the cellular target heme. A two-stage MD approach was employed for investigating the energies of heme−4-aminoquinoline drug interactions involving a simplified *in vacuo* study followed by more complex MD simulation in water.

Molecular Dynamics Simulations of the Heme−4-Aminoquinoline Complex *in Vacuo*.[29] Using DISCOVER the aminoquinoline under investigation was docked onto heme and a lowest energy conformation was generated. The geometry of the lowest observed energy complex of chloroquine with heme in these studies is in close agreement with the studies of Saterlee, where a similar $\pi-\pi$-orientation of the quinoline ring of chloroquine over the related porphyrin urohemin I was observed using ^{13}C NMR data.[30] The terminally charged nitrogen atom of the alkylamino side chain interacts with the heme carboxylates principally by electrostatic interactions rather than hydrogen bonding ($N_{diethyl}H-O_{heme} = 3.32$ Å) (Figure 3).

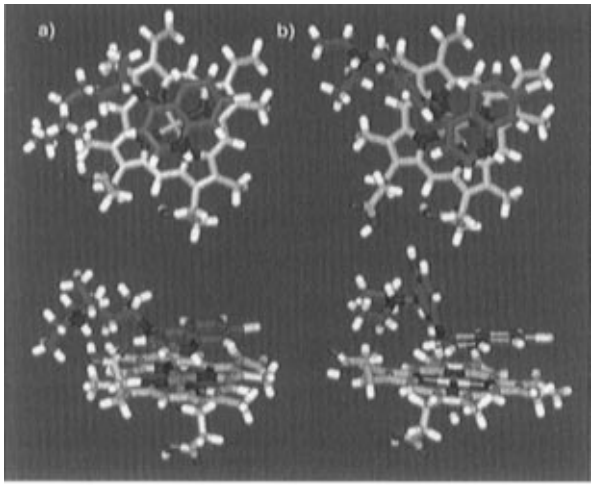

Figure 3. Lowest energy complexes of heme (*in vacuo*) with (a) chloroquine and (b) amodiaquine. Carbon atoms in heme are represented in gray and in green in both chloroquine and amodiaquine. Hydrogen atoms are in white, nitrogen in dark blue, and oxygen in red. Chlorine atoms are represented in pale green.

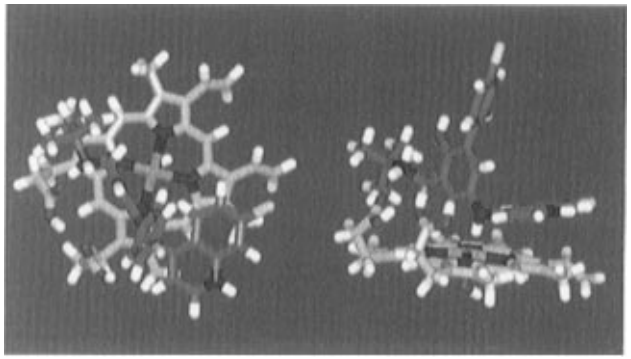

Figure 4. Lowest energy complexes of heme and tebuquine (*in vacuo*). The figure on the left is the view from above the complex, with the corresponding side-on view on the right. Atom labels are as in Figure 3.

A more detailed analysis was carried out on the interaction of tebuquine analogues with heme. Initial studies *in vacuo* indicated that the heme−drug complex is apparently stabilized by intermolecular H-bonding of the protonated side chain to one of the carboxylate functions in heme (Figure 4) with the quinoline nitrogen away from the central iron atom. The orientation of the amino side chain function in tebuquine is governed by intramolecular H-bonding between one of the protons on nitrogen with the lone pair on oxygen. This internal hydrogen bonding in tebuquine allows the side chain to adopt a conformation where the second proton on the charged ammonium atom can form a favorable hydrogen-bonding interaction with one of the carboxylates of heme.

Fluorine has widely been used in SAR studies as an isotere of the hydroxyl function.[43] Similarities between the electronegativities of fluorine and oxygen along with their similar bond lengths to carbon (different by only 0.04 Å) also indicate the potential utility of fluorine for oxygen substitution in producing active drug analogues. Our previous studies with amodiaquine have shown that replacement of the the hydroxyl function in amodiaquine with fluorine led to an analogue, fluoroamodi-

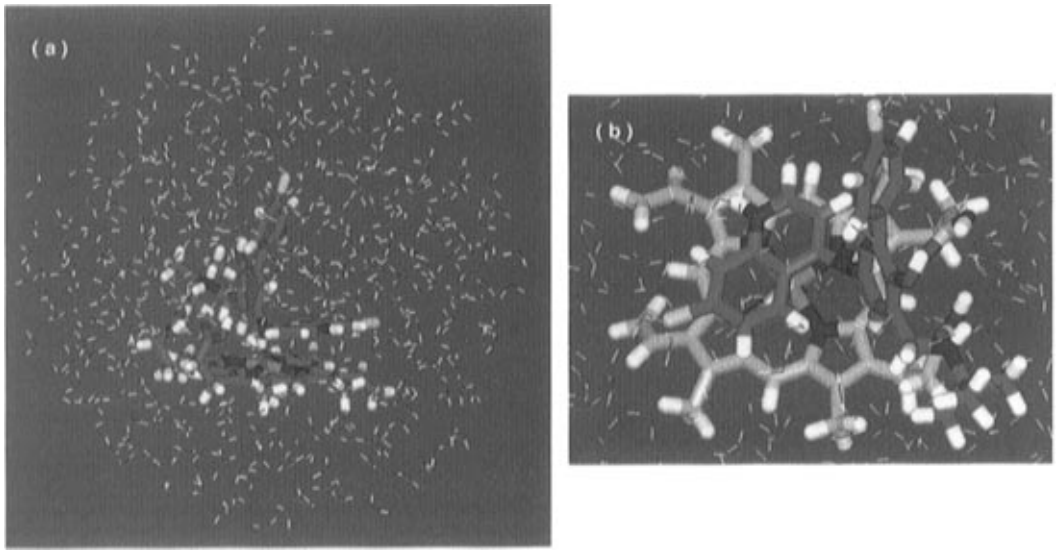

Figure 5. Heme−tebuquine-solvated complex: (a) snapshot at the beginning of the MD simulation; (b) snapshot after 40 ps. Atom labels are as in Figure 3.

aquine, that was potent both *in vitro* and *in vivo*.[7] It therefore seemed reasonable that replacement of the hydroxyl function in tebuquine would lead to potent antimalarials with activity against resistant strains of the malarial parasite. From Table 1 it is clear that activity has been reduced by fluorine substitution. This is also the case for dehydroxytebuquine (**7c**).

The interaction energies obtained for the drug−heme complexes are shown in Table 3, and the values are compared with antimalarial activity in the HB3 strain. Notably, dehydroxytebuquine has a high energy value, and this is reflected in low antimalarial activity. Fluorotebuquine, on the other hand, has an interaction energy that would suggest it should have similar potency to tebuquine if binding to heme is the only prerequisite for activity. As in the case of inter-nitrogen separation in the isolated molecules, there is no relationship between the "heme-bound" inter-nitrogen separation of a given analogue with drug activity.

Molecular Dynamics Simulations of the Heme−4-Aminoquinoline Complex in Water. In the studies described so far a constant dielectric coefficient was employed to simplify the computation, but it is potentially more useful in this case to carry out the simulations in a true water environment. Accordingly, a 4 Å shell of 400 water molecules was distributed evenly around selected heme/ligand structures, and the resulting system was subjected to molecular dynamics simulations for 100 ps at 298 K. Snapshots were made at the end of every 0.5 ps for a total of 200 structures. A snapshot of the heme−tebuquine complex is shown at the start of the simulation run in Figure 5. During the dynamics run it was observed that tebuquine adopts a conformation in water whereby the quinoline ring stacks above the porphyrin ring system with an additional hydrogen-bonding interaction with the carboxylates of heme and the proton on the side chain nitrogen (Figure 5, snapshot b).

This conformation was observed to be stable once formed in the dynamics run. Notably, out of the four analogues examined (Table 4), tebuquine had the most favorable interaction energy with heme, and it was noted that replacement of the hydroxyl function in tebuquine led to a decrease in interaction energy as in the *in vacuo* studies described above.

Table 5. Comparison of Cellular Accumulation Ratio (CAR) and Activity of 4-Aminoquinolines

drug	HB3 IC_{50} (nM)	SD ± mean	$1/IC_{50}$ (nM^{-1})	CAR
chloroquine (**1**)	9.75	2.75	0.102	1859
desethylchloroquine (**1a**)	17	0.6	0.059	682
amodiaquine (**2**)	3.7	0.8	0.270	12 613
desethylamodiaquine (**2a**)	4.5	2.3	0.222	6407
amopyroquine (**2b**)	1.7	0.7	0.588	39 560
N-tert-butylamodiaquine (**2c**)	3.7	0.9	0.270	21 081
5′-fluoroamodiaquine (**2d**)	55.2	2.9	0.018	1514
2′,6′-difluoroamodiaquine (**2e**)	47.3	2.5	0.021	922
dehydroxyamodiaquine (**2f**)	16.2	2.1	0.061	3089
tebuquine (**5**)	0.9	0.3	1.111	70 156
fluoroamodiaquine (**6**)	31.9	3.5	0.032	1711
fluorotebuquine (**7a**)	61.6	4.1	0.016	1081
dehydroxytebuquine (**7c**)	56.6	1.8	0.0176	1200

The essential feature or principle binding interactions in water appears to be planar $\pi-\pi$-stacking for amodiaquine, whereas for tebuquine, a combination of hydrogen bonding to the side chain carboxylates of heme and $\pi-\pi$-stacking over the porphyrin ring system are the most favorable mode of interaction with the large *p*-chlorophenyl function positioned away from the bonding sites. It is clear that the *N-tert-butyl function and hydroxyl are important for maximal activity* and that this fact is of potential importance *in the design of novel Mannich base antimalarials*.[44]

In this study, comparisons of interaction energies of the aminoquinoline−heme complex have been examined in an attempt to explain differences in potency brought about by the replacement of the 4′-hydroxyl in tebuquine. However, we must take into account that these chemical changes will also affect the physicochemical parameters of the drug that are relevant to cellular accumulation within the parasite. The cellular accumulation ratio (CAR) of the tebuquine analogues and related 4-aminoquinolines is shown in Table 5. It can be seen that fluorotebuquine accumulates within the parasite significantly less than tebuquine. Thus, although the energetics of heme binding may be similar for these agents, the fact that different quantities of drug reach the target site may explain the observed differences in

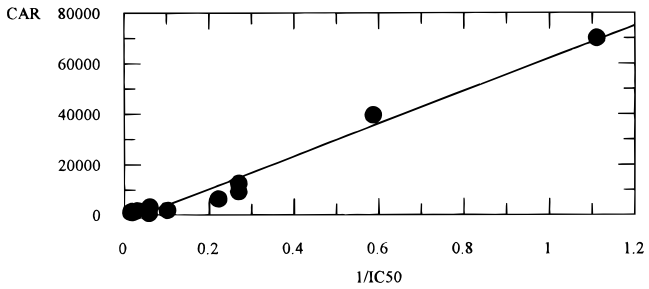

Figure 6. Graph of cellular accumulation ratio vs the $1/IC_{50}$.

activity observed. This factor is further underlined by the observation that although amodiaquine and dehydroxyamodiaquine have similar interaction energies in the water simulation studies, the latter antimalarial has lower cellular accumualtion and hence lower drug potency.

To stress the importance of cellular accumulation as an important component of drug activity, measurement of the cellular accumulation ratio of a total of 12 4-aminoquinolines was carried out (Table 5). Accumulation was found to be significantly correlated with the reciprocal of drug IC_{50} ($r = 0.98$) (Figure 6). It is therefore apparent that the combination of high accumulation and favorable heme binding appears to be important for high activity in the 4-aminoquinoline class of drugs.

Summary and Conclusion

Novel more direct synthetic routes have been developed for the synthesis of tebuquine, fluorotebuquine, and dehydroxytebuquine. The replacement of the 4-hydroxyl function with either fluorine or hydrogen led to a loss in activity against the chloroquine sensitive HB3 strain of the parasite. Molecular modeling of this set of aminoquinolines alongside amodiaquine and chloroquine suggests that inter-nitrogen separation in this class of drugs ranges between 9.3 and 9.8 Å in their isolated diprotonated form and between 7.52 and 10.21 Å in the heme−drug complex. Furthermore, all of the aminoquinolines under investigation are capable of binding to heme with favorable energy interactions. Studies on the molecular interaction of tebuquine with heme in an aqueous environment suggest that the 4-hydroxy function in tebuquine allows favorable orientation of the alkylamino function for hydrogen bonding to the carboxylates in heme. The complex is also stabilized by hydrophobic interactions between the quinoline ring and the porphyrin ring system of heme. In this limited series the energy values *E* of the "heme−4-aminoquinoline interaction" do not directly correlate with the observed antimalarial potencies but do provide insight into the geometry and functional groups involved in the interaction. The data suggest that the incorporation of a *p*-chlorophenyl function at the 3′-position of amodiaquine and the incorporation of a *tert*-butylamino group improve activity, potentially by enhanced accumulation within the parasite food vacuole and more favorable heme binding. When considering the effects of small chemical changes on the antimalarial activity of agents of this type, it is important to consider the cellular accumulation since differences in this latter parameter will obviously affect the available amount of drug to bind at the proposed binding site. Further work on correlating heme binding interaction energies using various water models is underway and will not only include a larger data set but also take into consideration the CAR factor. Studies of this type may aid in the future design of aminoquinoline antimalarials with the "hemoglobin degradation" pathway and heme as a potential target for the rational design of novel antimalarial compounds.

Experimental Section

Antimalarial Testing. Two strains of *P. falciparum* from Thailand were used in this study: (a) the uncloned K1 strain which is known to be chloroquine resistant and (b) the HB3 strain which is sensitive to all antimalarials. Parasites were maintained in continuous culture using a method derived from that of Jensen and Trager.[21] Cultures were maintained in culture flasks containing human erythrocytes (2−5%) with parasitemia ranging from 0.1% to 10% suspended in RPMI 1640 medium supplemented with 25 mM HEPES buffer, 32 mM $NaHCO_3$, and 10% human serum (complete medium). Cultures were gassed with a mixture of 3% O_2, 4% CO_2, and 93% N_2.

Antimalarial activity was assessed using an adaptation of the 48 h sensitivity assay of Desjardins et al.[22] using [^{3}H]-hypoxanthine incorporation as an assessment of parasite growth. Stock drug solutions were dissolved in 100% ethanol and diluted to an appropriate concentration with complete medium (final concentrations contained less than 1% ethanol). Assays were performed in sterile 96-well microtiter plates, each well containing 100 μL of medium which was seeded with 10 μL of a parasitized red blood cell mixture to give a resulting initial parasitemia of 1% with a 5% hematocrit. Control wells (which constituted 100% parasite growth) consisted of the above, with the omission of the drug.

After 24 h incubation at 37 °C, 0.5 μCi of hypoxanthine was added to each well. After a further 24 h incubation the cells were harvested onto filter mats, dried overnight, placed in scintillation vials with 4 mL of scintillation fluid, and counted on a liquid scintillation counter.

IC_{50} values were calculated by interpolation of the probit transformation of the log dose−response curve. Each compound was tested in triplicate to ensure reproducibility of the results. The measured IC_{50} is lineraly related to the size of the initial inoculum. Greater inoculum sizes give higher IC_{50} values due to depletion of drug from the medium. IC_{50} values were measured at a range of inoculum sizes, and the relationship was extrapolated to give the IC_{50} at a inoculum size of zero, i.e., no medium depletion. This value is termed the absolute IC_{50} (Table 1). Accumulation ratio was then calculated from the relationship:

$$\mathrm{CAR} = \frac{IC_{50}(\text{measured}) - IC_{50}(\text{absolute})}{IC_{50}(\text{absolute}) \times \text{fractional vol of PBRC}}$$

Chemistry. 4-Chlorophenylboronic acid, tetrakis(triphenylphosphine)palladium(0), boron tribromide (1 M in dichloromethane), 2-amino-5-nitrotoluene, and fluoroboric acid were obtained from Aldrich Chemical Co., Gillingham, Dorset, England. Merck Kieselgel 60 F 254 precoated silica gel plates for TLC were obtained from BDH, Poole, Dorset, U.K.

Column chromatography was carried out on Merck 938S silica gel. Infrared (IR) spectra were recorded in the range 4000−600 cm^{-1} using a Perkin Elmer 298 infrared spectrometer. Spectra of liquids were taken as films. Sodium chloride plates (Nujol mull) and solution cells (dichloromethane) were used as indicated.

Proton NMR spectra were recorded using Perkin Elmer R34 (220 MHz) and Bruker (400 and 200 MHz) NMR spectrometers. Solvents are indicated in the text, and tetramethylsilane was used as an internal reference. Mass spectra were recorded at 70 eV using a VG7070E mass spectrometer. The samples were introduced using a direct insertion probe. In the text the molecular ion (M^+) is given followed by peaks corresponding to major fragment losses with intensities in parentheses.

Melting points (mp) were determined on a Koffler hot stage apparatus and are uncorrected. Unless otherwise stated petroleum ether refers to petroleum spirit, bp 40−60 °C. Solvents were purified where necessary by standard procedures. Microanalysis was carried out by the University of Liverpool Microanalysis Laboratory.

3-Bromo-4-methoxyacetanilide (8). 4-Methoxyacetanilide was brominated using the conditions of Lauer.[19] The crude bromide was recrystallized from aqueous ethanol: ^{1}H NMR ($CDCl_3$, 200 MHz) δ 7.67 (1H, d, J_{H-H} = 2.75 Hz, Ar-H), 7.43 (1H, dd, J_{H-H} = 9.00 Hz, = 2.75 Hz, Ar-H), 7.24 (1H, s, *NH*COCH$_3$), 6.85 (1H, d, J_{H-H} = 9.00 Hz), 3.89 (3H, s, -OCH$_3$), 2.15 (3H, s, NHCO*CH*$_3$), 2.70 (2H, t, N*CH*$_2$CH$_2$OH), 2.61 (2H, q, N*CH*$_2$CH$_3$), 1.10 (3H, t, NCH$_2$*CH*$_3$); MS *m*/*z* 245/243 (M$^+$, 70), 203/201 (84), 106 (29). Anal. ($C_9H_{10}NO_2Br$), C,H,N.

3-(4′-Chlorophenyl)-4-methoxyacetanilide. 3-Bromo-4-methoxyacetanilide (1.47 g, 6.02 mmol) was dissolved in toluene (15 mL), and sodium carbonate (6 mL, 2 M solution) and ethanol (4 mL) were added. 4-Chlorophenylboronic acid (1.02 g, 6.70 mmol) was then added to the mixture followed by tetrakis(triphenylphosphine)palladium(0) (0.20 g, 0.18 mmol). The apparatus was charged with nitrogen and the reaction mixture heated under reflux for 5 h. Saturated brine was added (20 mL) and the mixture extracted with dichloromethane. The solvent was removed under reduced pressure and the residue subjected to column chromatography (silica gel, methanol / dichloromethane, 1:5) to give the product as a white solid: 1.32 g, 80%; ^{1}H NMR δ 7.30−7.50 (6H, m, Ar-H (RC$_6$*H*$_4$Cl, MeO-C$_6$*H*$_4$-NHCOCH$_3$)), 7.20 (1H, s, *NH*COCH$_3$), 6.93 (1H, d, J_{H-H} = 2.75 Hz, Ar-H), 3.93 (3H, s, -OCH$_3$), 2.10 (3H, s, NHCO*CH*$_3$); MS *m*/*z* 275 (M$^+$, 37), 233 (31), 183 (100); HRMS 275.071 09, ($C_{15}H_{14}NO_2Cl$ requires 275.071 29). Anal. ($C_{15}H_{14}NO_2Cl$), C,H,N.

3-(4′-Chlorophenyl)-4-hydroxyacetanilide. Boron tribromide (1 M in dichloromethane, 10 mmol) was added to a stirred suspension of 3-(4′-chlorophenyl)-4-methoxyacetanilide (2.00 g, 7.60 mmol) in dry dichloromethane (100 mL) under nitrogen, and the resulting mixture was allowed to stir at room temperature overnight. Water (75 mL) was added to hydrolyze the excess of boron tribromide, and the solution was allowed to stir for a further 30 min. The dichloromethane layer was separated and the water layer extracted three times with ethyl acetate (3 × 75 mL). The combined organic layers were dried ($MgSO_4$) and evaporated. The product was purified by flash column chromatography using dichloromethane/ethyl acetate (9:1) as eluent to give the phenol as a white crystalline product: mp 135−137 °C (lit.[2] mp 135 °C); ^{1}H NMR ($CDCl_3$, 200 MHz) δ 7.51−7.90 (6H, m, Ar-H (RC$_6$*H*$_4$Cl, HO-C$_6$*H*$_2$-NHCOCH$_3$)), 7.01 (1H, d, J_{H-H} = 9.00 Hz, Ar-H), 2.22 (3H, s, NHCO*CH*$_3$); MS *m*/*z* 261 (M$^+$, 76), 219 (100), 184 (35); HRMS 261.055 56 ($C_{14}H_{12}NO_2Cl$ requires 261.055 63). Anal. ($C_{14}H_{12}NO_2Cl$) C,H,N.

Tebuquine (5). 3-(4′-Chlorophenyl)-4-hydroxyacetanilide (1.00 g, 3.83 mmol) was allowed to react in a Mannich reaction (*tert*-butylamine, 0.41 g, and formaldehyde, 0.43 g) to give 3-(4′-chlorophenyl)-4-hydroxy-5-[(*tert*-butylamino)methyl]acetanilide as a white crystalline solid following chromatography (dichloromethane/methanol, 9:1): ^{1}H NMR ($CDCl_3$, 200 MHz) δ 7.60−7.00 (5H, m, Ar-H (RC$_6$*H*$_4$Cl, HO-C$_6$*H*$_2$-NHCOCH$_3$)), 7.01 (1H, d, J_{H-H} = 2.75 Hz, Ar-H), 4.12 (2H, s, CH$_2$NtBu), 2.10 (3H, s, NHCO*CH*$_3$), 1.15 (9H, s, tBu).

The amide function was hydrolyzed and the resulting aminophenol coupled with 4,7-dichloroquinoline to give the required product tebuquine as a yellow solid following chromatography using dichloromethane/methanol. The dihydrochloride salt was prepared by dissolving the free base in ethanolic hydrogen chloride (5 mL) followed by the addition of ether: mp (free base) 227−229 °C (lit.[2] mp 228 °C); ^{1}H NMR (CD$_3$OD, 200 MHz) δ 8.56 (1H, d, J_{H-H} = 8.80 Hz, Ar-H), 8.39 (1H, dd, J_{H-H} = 6.60, 2.75 Hz, Ar-H), 7.95 (1H, d, J_{H-H} = 2.20 Hz), 7.70 (1H, dd, J_{H-H} = 7.0, 2.20 Hz), 7.52 (5H, m, Ar-H), 7.38 (1H, m, Ar-H), 6.94 (1H, d, J_{H-H} = 8.80 Hz, Ar-H), 4.25 (2H, s, CH$_2$NtBu), 1.55 (9H, s, tBu). Anal. ($C_{26}H_{25}Cl_2N_3O$)·2HCl·0.5H$_2$O) C,H,N.

3-(4′-Chlorophenyl)-4-hydroxy-5-[(diethylamino)methyl]-acetanilide. 3-(4′-Chlorophenyl)-4-hydroxyacetanilide (2.61 g, 10 mmol) was subjected to a Mannich reaction with diethylamine (0.87 g, 12 mmol) and formaldehyde (0.90 g, 12 mmol) in ethanol. After refluxing for 5 h the solvent was removed under reduced pressure and the residue subjected to column chromatography (ethyl acetate) to give the product as a white solid (3.00 g, 86%): ^{1}H NMR ($CDCl_3$, 200 MHz) δ 7.10−7.60 (6H, m, Ar-H (RC$_6$*H*$_4$Cl, C$_6$*H*$_2$)), 3.79 (2H, s, -C*H*$_2$N), 2.63 (4H, q, N*CH*$_2$CH$_3$), 2.10 (3H, s, NHCOC*H*$_3$), 1.11 (6H, t, NCH$_2$*CH*$_3$); MS *m*/*z* 346 (M$^+$, 19), 274 (21), 231 (28); HRMS 346.1449 ($C_{15}H_{14}NO_2Cl$ requires 346.144 81).

3′-(Chlorophenyl)amodiaquine (Amotebuquine) (7). The amide function of 3-(4′-chlorophenyl)-4-hydroxy-5-(diethylamino)acetanilide (1.73 g, 5 mmol) was hydrolyzed and coupled with 4,7-dichloroquinoline (0.98 g, 5 mmol) to give amotebuquine (2.10 g, 90%) as a yellow solid. The solid was recrystallized from acetonitrile and toluene to give the pure compound: mp 232−233 °C (lit.[2] mp 229−232 °C); ^{1}H NMR ($CDCl_3$, 200 MHz) δ 8.50 (1H, d, J_{H-H} = 4.95 Hz, Ar-H), 8.00 (1H, d, J_{H-H} = 1.65 Hz, Ar-H), 7.84 (1H, d, J_{H-H} = 9.35 Hz, Ar-H), 7.30−7.60 (5H, m, RC$_6$*H*$_4$Cl, C$_6$*H*$_2$), 7.15 (1H, d, J = 2.75 Hz, Ar-H), 6.94 (1H, d, J_{H-H} = 2.30 Hz, Ar-H), 6.70 (1H, d, J_{H-H} = 2.30 Hz, Ar-H), 6.63 (1H, s, NH), 3.83 (2H, s, -C*H*$_2$N), 2.67 (4H, q, N*CH*$_2$CH$_3$), 1.13 (6H, t, NCH$_2$*CH*$_3$); MS *m*/*z* 465 (M$^+$, 2), 394 (9); HRMS 465.136 93 ($C_{26}H_{25}N_3OCl_2$ requires 465.137 45). Anal. ($C_{26}H_{25}N_3OCl_2$) C, H, N.

2-Amino-3-bromo-5-nitrotoluene (9). 2-Amino-5-nitrotoluene (75 g, 0.50 mol) was dissolved by heating in concentrated HCl, and the solution was allowed to cool to room temperature. Bromine (87 g, 0.54 mol) was added dropwise over 2 h and the solution allowed to stir for an additional 1 h. The solution was filtered and the solid agitated with 1 l of 0.5M $NaHCO_3$ to hydrolyze the hydrochloride of the product. The insoluble base was filtered off and recrystallized from ethanol to give the product as a yellow solid (100 g, 85%): mp 174−175 °C; MS *m*/*z* 230/232 (M$^+$, 100), 202/200 (77), 104 (78); HRMS 229.968 85 ($C_7H_7N_2O_2Br$ requires 229.969 09); IR (Nujol mull) 3480, 3381, 2927, 2855, 1619, 1461, 1377, 1301, 1100. Anal. ($C_7H_7N_2O_2Br$) C, H, N.

2-Fluoro-3-bromo-5-nitrotoluene (10). 2-Amino-3-bromo-5-nitrotoluene (57.75 g, 0.25 mol) was dissolved in 110 mL of fluoroboric acid in a 400 mL beaker. The beaker was placed in an ice bath and the solution stirred with an efficient stirrer. A cold solution of sodium nitrite (17 g, 0.25 mol) in water (35 mL) was added dropwise. When the addition was complete the mixture was stirred for 15 min and filtered by suction on a sintered glass funnel. The solid diazonium salt was washed with fluoroboric acid, twice with ethanol, and several times with ether. The product was dried to give 57.57 g (70%).

Thermal Decomposition. Without further purification, the diazonium product was mixed with 150 g of acid-washed sand. The mixture was placed in a three-neck flask, and a nitrogen supply was attached in order to allow a constant flow of nitrogen through the apparatus during decomposition. The reaction was initiated by heating to 150 °C for 10 min. The vigorous reaction was allowed to continue until evolution of BF_3 gas had ceased. The nitrogen supply was removed and the dark mass allowed to cool. The residue was dissolved in dichloromethane (600 mL), and the sand was filtered off. The solvent was removed under reduced pressure, and the residue was purified by chromatography on alumina using dichloromethane as eluent to give the product (20 g, 40%) as a pale yellow solid: ^{1}H NMR ($CDCl_3$, 200 MHz) δ 8.31 (1H, dd, J_{H-F} = 4.95 Hz, J_{H-H} = 2.75 Hz, Ar-H), 8.06 (1H, dd, J_{H-F} = 4.95 Hz, J_{H-H} = 2.75 Hz, Ar-H), 2.42 (3H, d, J_{H-F} = 2.2 Hz, CH$_3$); IR (Nujol mull) 3096, 2958, 1578, 1534, 1466, 1377, 1347, 1307, 1269, 1222, 1205, 1091, 1038, 898, 743; MS *m*/*z* 233 (M$^+$, 44), 203 (14), 167 (15), 108 (100); HRMS 232.948 54 ($C_7H_5NO_2FBr$ requires 232.948 76).

2-Fluoro-3-(4′-chlorophenyl)-5-nitrotoluene. 2-Fluoro-3-bromo-5-nitrotoluene (3.00 g, 13 mmol) was coupled with 4-chlorophenylboronic acid using the conditions described for 3-(4′-chlorophenyl)-4-methoxyacetanilide. The product was purified using ethyl acetate/petroleum ether (1:5) to give the product as a white solid (2.50, 72%): ^{1}H NMR ($CDCl_3$, 200 MHz) δ 8.08−8.20 (2H, m, Ar-H), 7.48−7.55 (4H, m, Ar-H), 2.42 (3H, s, CH$_3$); IR (Nujol mull) 2944, 1594, 1522, 1461, 1377,

1296, 1237, 1209, 1094, 747; MS *m/z* 265 (M^+, 76), 183 (100), 163 (12); HRMS 265.031 04 ($C_{13}H_9NO_2FCl$ requires 265.030 58).

3-(4′-Chlorophenyl)-4-fluoro-5-[[(*tert*-butylamino)methyl]anilino]nitrobenzene. 2-Fluoro-3-(4′-chlorophenyl)-5-nitrotoluene (1.00 g, 3.77 mmol) was brominated with NBS (1.34 g, 7.54 mmol) and AIBN (catalytic) by heating in carbon tetrachloride for 8 h (TLC analysis revealed the completion of the reaction). The solvent was removed under reduced pressure, without further purification *tert*-butylamine (excess) was added with toluene (35 mL), and the reaction mixture was heated to reflux for 10 h under nitrogen. The reaction mixture was allowed to cool and filtered. The solvent was removed and the residue purified by flash column chromatography on silica gel using dichloromethane/methanol (95:5) as eluent to give the product as a pale yellow foam: ^{1}H NMR ($CDCl_3$, 200 MHz) δ 8.40 (1H, dd, J_{H-F} = 5.50 Hz, J_{H-H} = 2.75 Hz, Ar-H), 8.20 (1H, dd, J_{H-F} = 5.50 Hz, J_{H-H} = 2.75 Hz, Ar-H), 7.55 (4H, m, Ar-H, RC_6H_4Cl), 3.95 (2H, s, CH_2N), 1.23 (9H, s, tBu). Anal. ($C_{17}H_{18}NO_2FCl$).

Fluorotebuquine (7a). The nitro compound **16** (0.50 g, 1.48 mmol) was reduced using tin/HCl and the resulting amine coupled with 4,7-dichloroquinoline to give the required product as a yellow solid following column chromatography (dichloromethane/methanol, 8:2): mp 179 °C; ^{1}H NMR ($CDCl_3$, 200 MHz) δ 8.55 (1H, dd, J_{H-H} = 4.95 Hz, Ar-H), 8.02 (1H, dd, J_{H-H} = 2.20 Hz, Ar-H), 7.89 (1H, d, J_{H-H} 8.80 Hz, Ar-H), 7.31−7.51 (6H, m, RC_6H_4Cl, Ar-H), 7.20 (1H, dd, J_{H-H} = 6.05, 2.20 Hz), 6.85 (1H, d, J_{H-H} = 5.50 Hz), 3.85 (2H, s, CH_2NHtBu), 1.07 (9H, s, tBu); MS *m/z* 467 (M^+, 4.2), 455 (15), 452 (100), 395 (32), 380 (47), 360 (47), 227 (21), 170 (41), 162 (33); HRMS 467.131 53 ($C_{26}H_{24}N_3FCl_2$ requires 467.133 15). Anal. ($C_{26}H_{24}N_3FCl_2$) C,H,N.

3-(4′-Chlorophenyl)-4-fluoro-5-[(diethylamino)methyl]-nitrobenzene. 2-Fluoro-3-(4′-chlorophenyl)-5-nitrotoluene (**20**) (1.00 g, 3.77 mmol) was brominated with NBS (1.34 g, 7.54 mmol) and AIBN (catalytic) by heating in carbon tetrachloride as described for (**16**). The solvent was removed under reduced pressure, without further purification diethylamine (0.55 g, 7.54 mmol) was added with toluene (35 mL), and the reaction mixture was allowed to reflux for 10 h under nitrogen. The reaction mixture was allowed to cool and filtered. The solvent was removed and the residue purified by flash column chromatography on silica gel using dichloromethane/methanol (95:5) as eluent to give the product as a pale yellow foam (0.83 g, 65%): ^{1}H NMR ($CDCl_3$, 200 MHz) δ 8.43 (1H, dd, J_{H-F} = 6.05 Hz, J_{H-H} = 2.75 Hz, Ar-H), 8.19 (1H, dd, J_{H-F} = 6.05 Hz, J_{H-H} = 2.75 Hz, Ar-H), 7.43−7.50 (4H, m, Ar-H, RC_6H_4Cl), 3.71 (2H, s, -CH_2N), 2.60 (4H, q, NCH_2CH$_3$), 1.08 (6H, t, NCH$_2$$CH_3$); MS *m/z* 336 ($M^+$, 8), 321 (100), 264 (80), 183 (*73*); HRMS 336.103 77 ($C_{17}H_{18}N_2O_2ClF$ requires 336.104 10).

Fluoroamotebuquine (7b). 3-(4′-Chlorophenyl)-4-fluoro-5-[(diethylamino)methyl]nitrobenzene (0.50 g, 1.48 mmol) was dissolved in concentrated hydrochloric acid (5 mL), and an excess of tin turnings was added (ca. 1.40 g, 11.84 mmol). The mixture was stirred for 1 h and then heated for 45 min to complete the reduction. The mixture was allowed to cool and concentrated sodium hydroxide solution (80 mL) added. The amine was extracted with dichloromethane by several washings of the aqueous layer. The organic extracts were dried ($MgSO_4$), and the solvent was removed to give the amine as a pale yellow oil. The amine was dissolved in ethanol (15 mL) and 4,7-dichloroquinoline (0.20 g, 1 mmol) added. The ethanol solution was acidified (pH = 5.5) and then heated under reflux for 8 h. The product was obtained by basification and filtration. The solid product was dried and purified by column chromatography using dichloromethane/methanol (5:1) to give an off-white solid (0.52 g, 76%): ^{1}H NMR ($CDCl_3$, 200 MHz) δ 8.56 (1H, dd, J_{H-H} = 4.95 Hz, Ar-H), 8.04 (1H, d, J_{H-H} = 1.65 Hz, Ar-H), 7.93 (1H, d, J_{H-H} = 8.80 Hz, Ar-H), 7.40−7.60 (7H, m, Ar-H, RC_6H_4Cl), 6.90 (1H, d, J_{H-H} = 4.95 Hz), 3.72 (2H, s, -CH_2N), 2.65 (4H, q, NCH_2CH$_3$), 1.10 (6H, t, NCH$_2$$CH_3$); MS *m/z* 467 ($M^+$, 3), 452 (45), 396 (88), 380 (45), 227 (30), 170 (36), 162 (27). Anal. ($C_{26}H_{24}N_3FCl_2$) C, H, N.

3-Bromo-5-nitrotoluene. 2-Amino-3-bromo-5-nitrotoluene (5 g, 0.021 mol) was dissolved in ethanol (60 mL) and toluene (15 mL) in a 250 mL round-bottomed flask. Sulfuric acid (3.5 mL) was added and the solution gently heated in order to dissolve all of the starting material. When the clear solution boiled, the condenser and heat source were removed. Sodium nitrite (2.00 g) was added in two portions, and the condenser was reconnected while the reaction took place; additional heating was used to complete the reaction. The solution was allowed to cool down and placed in a refrigerator overnight. The crude product was filtered off and washed with ethanol and then water to remove sodium sulfate. The material was of sufficient purity for use in the next reaction: mp 87−90 °C; ^{1}H NMR ($CDCl_3$, 200 MHz) δ 8.16−8.20 (1H, m, Ar-H), 7.96−8.00 (1H, m, Ar-H), 7.64−7.68 (1H, m, Ar-H), 2.47 (3H, s, -CH_3); IR (Nujol mull) 2930, 1535, 1458, 1377, 1348, 1300, 879, 872, 839, 737; MS *m/z* 217/215 (M^+, 69/67), 169 (33), 89/90 (92/100); HRMS 214.958 04 ($C_7H_6NO_2Br$ requires 214.958 19).

3-(4′-Chlorophenyl)-5-nitrotoluene (11). 3-Bromo-5-nitrotoluene was subjected to the Suzuki reaction as described for compound **10**. The yield was 75%: mp 90 °C ; ^{1}H NMR ($CDCl_3$, 200 MHz), δ 8.22 (1H, s, Ar-H), 8.04 (1H, m, Ar-H), 7.68 (1H, m, Ar-H), 7.50 (4H, m, Ar-H), 2.60 (3H, s, -CH_3); IR (Nujol mull) 2918, 2856, 1526, 1490, 1459, 1376, 1362, 1291; MS *m/z* 247 (M^+, 100), 201 (17), 165 (60); HRMS 247.040 09 ($C_{13}H_{10}NO_2Cl$ requires 247.039 99).

3-[(*tert*-Butylamino)methyl]-5-(4′-chlorophenyl)-nitrobenzene. 3-(4′-Chlorophenyl)-5-nitrotoluene was brominated and allowed to react with *tert*-butylamine as described for **16**: mp 90−92 °C; ^{1}H NMR ($CDCl_3$, 200 MHz) δ 8.26 (1H, m, Ar-H), 8.22 (1H, m, Ar-H), 7.90 (1H, s, Ar-H), 7.50 (4H, m, Ar-H), 3.95 (2H, s, -CH_2N), 1.20 (9H, s, tBu); IR (Nujol mull) 2915, 2853, 1601, 1533, 1497, 1458, 1376, 1219, 1164; MS *m/z* 317 (M^+, 1), 303 (100), 246 (45), 165 (26). Anal. ($C_{17}H_{18}N_2O_2$-Cl) C,H,N.

Dehydroxytebuquine (7c). 3-[(*tert*-Butylamino)methyl]-5-(4′-chlorophenyl)nitrobenzene was reduced using tin/HCl as described in the synthesis of **7b**: ^{1}H NMR ($CDCl_3$, 200 MHz) δ 7.40 (4H, m, Ar-H), 6.90 (1H, m, Ar-H), 6.70−6.75 (m, 2H, Ar-H), 3.89 (2H, s, -CH_2N), 1.17 (9H, s, tBu); IR (Nujol mull) 3182, 2915, 2853, 1601, 1533, 1497, 1458, 1376, 1219, 1164; MS *m/z* 288 (M^+, 11), 273 (68), 216 (100), 180 (24); HRMS 288.139 59 ($C_{17}H_{21}N_2Cl$ requires 288.139 31).

The amine was coupled with 4,7-dichloroquinoline as described for **7b** to give the product dehydroxytebuquine (**7c**) as a yellow solid following column chromatography on silica gel, 10% MeOH, 90% dichloromethane: ^{1}H NMR ($CDCl_3$, 200 MHz) δ 9.59 (1H, s, NH), 9.01 (1H, d, J_{H-H} = 9.40 Hz), 8.55 (1H, d, J_{H-H} = 6.58 Hz, Ar-H), 8.18 (d, J_{H-H} = 2.20 Hz, Ar-H), 8.10 (1H, s, Ar-H), 7.85 (4H, m, Ar-H, RC_6H_4Cl), 7.60 (1H, d, J_{H-H} = 8.80 Hz, Ar-H), 7.20 (1H, d, J_{H-H} = 7.14 Hz), 4.20 (2H, s, -CH_2N), 1.41 (9H, s, tBu); MS *m/z* 449 (M^+, 10), 434 (100), 377 (30), 362 (27); HRMS 449.142 12 ($C_{26}H_{25}N_3Cl_2$ requires 449.142 55).

Acknowledgment. We thank the Wellcome Trust (B.K.P., S.A.W.), M.R.C. (S.R.H.), Roche (Welwyn) (P.M.O.), and the University of Liverpool for financial support. The authors also thank Dr. J. L. Maggs for EI+ mass spectrometry and Lawrence Bishop (Wellcome Vacation Studentship) and Sandra Lust for technical assistance. The authors also thank Prof. R. J. Abraham (Liverpool University) for helpful discussion.

References

(1) *WHO Practical Chemotherapy of Malaria*; Technical Report Series No. 805; World Health Organization: Geneva, 1990.

(2) Hawley, S. R.; Bray, P. G.; O'Neill, P. M.; Park, B. K.; Ward, S. A. The Role of Drug Accumulation in 4-Aminoquinoline Antimalarial Potency: The Influence of Structural Substitution and Physicochemical Properties. *Biochem. Pharmacol.* **1996**, *52*, 723−733.

(3) Werbel, L. M.; Cook, P. D.; Elslager, E. F.; Hung, J. H.; Johnson, J. L.; Keston, S. J.; McNamara, D. J.; Ortwine, D. F; Worth, D. F., Synthesis, Antimalarial Activity and Quantitative Structure-Activity Relationships of Tebuquine and a Series of Related 5-[(7-chloro-4-quinolinyl)amino]-3-[(alkylamino)methyl][1,1′-biphenyl]-2-ols and N-oxides. *J. Med. Chem.* **1986**, *29*, 924−939.

(4) Lind, D. E.; Levi, J. A.; Vincent, P. C. Amodiaquine Induced Agranulocytosis; Toxic Effects of Amodiaquine in Bone Marrow Culture In Vitro. *Br. Med. J.***1973**, *1*, 458−460.
(5) Maggs, J. L.; Kitteringham, N. R.; Park, B. K. Drug Protein Conjugates-XIV. Mechanism of Formation of Protein Arylating Intermediates From Amodiaquine a Myelotoxin and Hepatotoxin in Man. *Biochem. Pharmacol.* **1988**, *37*, 303−311.
(6) Harrison, A. C.; Kitteringham, N. R.; Clarke, J. B.; Park, B. K. The Mechanism of Bioactivation and Antigen Formation of Amodiaquine in the Rat. *Biochem. Pharmacol.* **1992**, *43*, 1421−1430.
(7) O'Neill, P. M.; Harrison, A. C.; Storr, R. C.; Hawley, S. R.; Ward, S. A.; Park, B. K. The Effect of Fluorine Substitution on the Metabolism and Antimalarial Activity of Amodiaquine. *J. Med. Chem.* **1994**, *37*, 1362−1370.
(8) Ruscoe, J. E.; Jewell, H.; Maggs, J. L.; O'Neill, P. M.; Storr, R. C.; Ward, S. A.; Park, B. K. The Effect of Chemical Substitution on the Metabolic Activation, Metabolic Detoxication, and Pharmacological Activity of Amodiaquine in the Mouse. *J. Pharmacol. Exp. Ther.* **1995**, *273*, 393−404.
(9) Jewell, H.; Maggs, J. L.; Ruscoe, J. E.; Harrison, A. C.; O'Neill, P. M.; Ruscoe, J. E.; Park, B. K. The Role of Hepatic Metabolism in the Bioactivation and Detoxication of Amodiaquine. *Xenobiotica* **1995**, *25*, 199−217.
(10) Tingle, M. D.; Jewell, H.; Maggs, J. L.; O'Neill, P. M.; Park, B. K. The Bioactivation of Amodiaquine by Human Polymorphonuclear Leucocytes In Vitro: Chemical Mechanisms and the Effects of Fluorine Substitution, *Biochem. Pharmacol.* **1995**, *50*, 1113−1119.
(11) O'Neill, P. M.; Tingle, M. D.; Mahmud, R.; Storr, R. C.; Ward, S. A.; Park, B. K. The Effect of Fluorine Substitution on the Haemotoxicity of Primaquine. *Bio. Med. Chem. Lett.* **1995,** *20***,** 2309−2314.
(12) Hawley, S. R.; Bray, P. G.; O'Neill, P. M.; Naisbitt, D. J.; Park, B. K.; Ward, S. A. Manipulation of the N-alkyl Substituent in Amodiaquine to Overcome the Verapamil Sensitive Chloroquine Resistance Component. *Antimicrob. Chemother.* **1996**, in press.
(13) Chou, A. C.; Chevli, R.; Fitch, C. D. Ferriprotoporphyrin IX Fulfills the Criteria for Identification as the Chloroquine Receptor of Malaria Parasites. *Biochemistry* **1980**, *19*, 1543−1549.
(14) Blauer, G.; Akkawi, M.; Bauminger, E. R. Further Evidence for the Interaction of the Antimalarial Drug Amodiaquine with Ferriprotoporphyrin IX. *Biochem. Pharmacol.* **1993**, *46*, 1573−1576.
(15) Ginsburg, H.; Krugliak, M. Quinoline Containing Antimalarials: Mode of Action, Drug-Resistance and Its Reversal. An Update with Unresolved Puzzles. *Biochem. Pharmacol.* **1992**, 43, 63−70.
(16) Geary, T. G.; Divo, A. D.; Jensen, J. B.; Zangwill, M.; Ginsburg, H. Kinetic modeling of the Response of Plasmodium falciparum to Chloroquine and its Experimental Testing In Vitro. Implications for Mechanism of Action and Resistance to the Drug. *Biochem. Pharmacol.* **1990**, *40*, 685−691.
(17) Fanta, P. E. The Ullman Synthesis of Biaryls. *Chem. Rev.* **1946**, *38*, 139.
(18) Hill, H. B.; Hale, W. *J. Am. Chem. Soc.* **1905**, *33*, 1.
(19) Lauer, W. L.; Rondestvedt, C.; Arnold, R. T.; Drake, N. L.; Van Hook, J.; Tinker, J. Some Derivatives of 8-Aminoquinoline. *J. Am. Chem. Soc.* **1946**, *68*, 1546.
(20) Miyaura, N.; Yanagi, T.; Suzuki, A. The Palladium-Catalyzed Cross-Coupling Reaction of Phenylboronic Acid with Haloarenes in the Presence of Bases. *Synth. Commun.* **1981**, *11*, 513−519.
(21) Jensen, J. B.; Trager, W. Plasmodium Falciparum in Culture; Use of Outdated Erythrocytes and Description of the Candle Jar Method. *J. Parasitol.* **1977**, 63, 883−886.
(22) Desjardins, R. E.; Canfield, J.; Haynes, D.; Chulay, D. J. Quantitative Assessment of Antimalarial Activity In Vitro by a Semi-automated Microdilution Technique. *Antimicrob. Agents. Chemother.* **1979**, *16*, 710−718.
(23) Koh, H. L.; Go, M. L.; Ngiam, T. L.; Mak, J. W. Conformational and Structural Features Determining In Vitro Antimalarial Activity in Some Indolo[3,2-c]quinolines, anilinoquinolines and tetrahydroindolo[3,2-d] benzazepeines. *Eur. J. Med. Chem.* **1994**, *29*, 107−113.
(24) Polowin, J.; Poer Baird, M. C. Extensions of the Applicability of the MMX Molecular modeling System in the Determination of Barriers to Rotation of pi-Bonded Ligands. *Can. J. Chem.* **1995**, *73*, 1078−1083.
(25) Stewart, J. J. P. Mopac - A Semiempirical Molecular-Orbital Program. *J. Comput.-Aided Mol. Des.* **1990**, *4*, 1−45.
(26) Discover, 1993, Biosym Technologies Inc., San Diego, CA 92121-2777.
(27) Barlow, S.; Rohl, A. L.; O'Hare, D. Molecular-Mechanics Study of Oligomeric Models for Polyferrocenylsilanes Using the Esff Forcefield. *Chem. Commun.* **1996**, 256. For another example of molecular modeling on hemes, see: Ranghino, G.; Fantucci, P. Molecular modeling of Heme Peptides-Molecular Dynamics Simulation of Microperoxidase. *Israel Chem.* **1994**, *34*, 239−244.
(28) Rodighiero, P.; Guiotto, A.; Chilin, A.; Bordin, F.; Baccicheti, F.; Carlassare, F.; Vedaldi, D.; Caffieri, S.; Pozzan, A.; Dall'Acqua, F. D. Angular Furoquinolinones, Psoralen Analogs: Novel Antiproliferative Agents for Skin Diseases. Synthesis, Biological Activity, Mechanism of Action, and Computer-Aided Studies. *J. Med. Chem.* **1996**, *39*, 1293−1302. See also *J. Mol. Graph.* **1993**, *13*, 215.
(29) Wang, S.; Kazanietz, M. G.; Blumberg, P. M.; Marquez, V. E., Milne, G. W. A., Molecular modeling and Site-Directed Mutagenesis Studies of a Phorbol Ester-Binding Site in Protein Kinase C. *J. Med. Chem.* **1996**, *39*, 2541−2553.
(30) Constantinindis, I.; Saterlee, J. D. UV-Visible and Carbon NMR Studies of Chloroquine Binding to Urohemin I Chloride and Uroporphyrin I in Aqueous Solutions. *J. Am. Chem. Soc.* **1988**, *110*, 4391−4395.
(31) Moreau, S.; Perly, B.; Chachaty, C.; Deleuze, C. A Nuclear Magnetic Resonance Study of the Interactions of Antimalarial Drugs with Porphyrins. *Biochim. Biophys. Acta* **1985**, *840*, 107−116.
(32) For an excellent perspective, see: Ajay; Murcko, M. A. Computational Methods to Predict the Binding Free Energy in Ligand Recptor Complexes. *J. Med. Chem.* **1995**, *38*, 4953−4967. The free energy of binding is an additive interaction of different energy terms described by the so-called "master equation" which is written as

$$G_{\text{bind}} = \Delta G_{\text{solvent}} + \Delta G_{\text{conf}} + \Delta G_{\text{int}} + \Delta G_{\text{motion}}$$

This equation considers the solvent, changes in conformation in ligand and receptor, the interaction energy, and the motion in the receptor and ligand once proximal. As described by Ajay the interaction energy for a drug binding to ligand is an enthalpic contribution written as

$$G_{\text{int}} = \Delta E_{\text{int}} = E_{\text{total}} - E_{\text{free protein}} - E_{\text{ligand}}$$

(33) Yennawar, H. P.; Viswamitra, M. A. Steric and Rotational Constraints in the X-Ray Structure of the Antimalarial Drug Amodiaquine. *Curr. Sci.* **1991**, *61*, 39−43.
(34) (a) Chou, A. C.; Fitch, C. D. Mechanism of Hemolysis Induced by Ferriprotoporpyrin IX. *J. Clin. Invest.* **1981**, 672−677. (b) Sugioka, Y.; Suzuki, M.; Sugioka, K.; Nakano, M. A Ferriprotoporphyrin IX-Chloroquine Complex Promotes Membrane Phospholipid Peroxidation. *FEBS Lett.* **1987**, *223*, 251−254.
(35) Orjih, A. U.; Banyal, H. S.; Chevli, R.; Fitch, C. D. Hemin Lyses Malaria Parasites. *Science* **1981**, *214*, 667−669.
(36) Slater, A. F. G.; Swiggard, W. J.; Orton, B. R.; Flitter, W. D.; Goldberg, D. E.; Cerami, A.; Henderson, G. B. An Iron-Carboxylate Bond Links the Heme Units of Malaria Pigment. *Proc. Natl. Acad. Sci.* U.S.A. **1991**, *88*, 325−329.
(37) Slater, A. F. G. Malaria Pigment. *Exp. Parasitol.* **1992**, *74*, 362−365.
(38) Warhurst, D. C. Antimalarial Interaction with Ferriprotoporphyrin IX Monomer and its Relationship to Activity of Blood Schizonticides. *Ann. Trop. Med. Parasitol.* **1987**, *81*, 65−67.
(39) Ginsburg, H.; Krugliak, M. Effects of Quinoline Containing Antimalarials on the Erythrocyte Membrane and Their Significance to Drug Action on Plasmodium Falciparum. *Biochem. Pharmacol.* **1988**, *37*, 2013−2018.
(40) Ginsburg, H.; Demel, R. A. Interactions of Hemin, Antimalarial Drugs and Hemin-Antimalarial Complexes with Phopolipid Monolayers. *Chem. Phys. Lipid* **1984**, *35*, 331−347.
(41) For details of the the X-ray structure of hemin chloride see *Acta Crystallogr.* **1965**, *18*, 663. Intramolecular distances of O in the carboxylates CO_2^- from the central Fe(III) in hemin chloride are as follows: distance $d_1 = 8.39$ Å, distance $d_2 = 7.66$ Å, distance $d_3 = 8.14$ Å, and distance $d_4 = 8.65$ Å.
(42) Yayon, A.; Cabantchik, Z. I.; Ginsburg, H. Identification of the Acidic Compartment of Plasmodium Falciparum-Infected Human Erythrocytes as the Target of the Antimalarial Drug Chloroquine. *EMBO J.* **1984**, *11*, 2695−2700.
(43) Park, B. K.; Kitteringham, N. R. Effects of Fluorine Substitution on Drug Metabolism: Pharmacological and Toxicological Implications. *Drug Metab. Rev.* **1994**, *26*, 605−643.
(44) For a detailed examination of the effect on antimalarial activity of replacing the *N*-diethylamino of amodiaquine with the N-tert-butyl group, see: Hawley, S. R.; Bray, P. G.; O'Neill, P. M.; Naisbitt, D. J.; Park, B. K.; Ward, S. A. Manipulation of the N-Alkyl Substituent in Amodiaquine to Overcone the Verapamil Sensitive Chloroquine Resistance Mechanism. *Antimicrob. Agents Chemother.* **1996**, *40*, 2345−2349.

JM960370R